Two–body heating in numerical
galaxy formation experiments

Matthias Steinmetz[1,2] and Simon D.M. White[1]

[1]Max–Planck–Institut für Astrophysik, Postfach 1523, 85740 Garching, Germany

[2]Department of Astronomy, University of California, Berkeley, CA 94720, USA

Abstract

We show that discreteness effects related to classical two-body relaxation produce spurious heating of the gaseous component in numerical simulations of galaxy formation. A simple analytic calculation demonstrates that this artificial heating will dominate radiative cooling in any simulation where the mass of an individual dark matter particle exceeds a certain critical value. This maximum mass depends only on the cooling function of the gas, on the fraction of the material in gaseous form, and (weakly) on typical temperatures in the gas. It is comparable to, or smaller than, the dark matter particle masses employed in most published simulations of cosmological hydrodynamics and galaxy formation. Any simulation which violates this constraint will be unable to follow cooling flows, although catastrophic cooling of gas may still occur in regions with very short cooling times. We use a series of N–body/smoothed particle hydrodynamics simulations to explore this effect. In simulations which neglect radiative cooling, two–body heating causes a gradual expansion of the gas component. When radiative effects are included, we find that gas cooling is almost completely suppressed for dark matter particle masses above our limit. Although our test simulations use smoothed particle hydrodynamics, similar effects, and a similar critical mass, are expected in any simulation where the dark matter is represented by discrete particles.

1 Introduction

Over the last twenty years our understanding of structure formation has benefitted substantially from numerical N-body simulations. It is now clear that such simulations provide a robust and efficient, though sometimes computationally expensive tool to obtain approximate solutions for the evolution of a collisionless self-gravitating "fluid" from cosmologically relevant initial conditions (Efstathiou et al 1985). Although such cosmological N–body simulations can now be performed using particle numbers in excess of 10^7, and

1

can follow density contrasts over a range of 10^6, this still turns out to be barely sufficient to address questions related to the formation of galaxies in a proper cosmological context. Current observational data appear to favour models in which structure is built up hierarchically, and so it is of particular interest to ask how numerical resolution affects the mass hierarchy at the low mass end. It appears that while the detailed inner structure of halos can only be analyzed reliably if they contain at least several hundred particles, the distribution of halos and their total masses are reasonably represented for halos with ten or more particles (e.g. Efstathiou et al 1988). This convergence is of major importance because it means that simulations performed with $\sim 10^7$ particles can reliably resolve the halos of galaxies like the Milky Way while simultaneously covering a large enough region (a few hundreds of Mpc) to allow a statistical comparison with galaxy surveys. The most serious limitation of such models is the fact that the formation of real galaxies was clearly strongly affected by a wide variety of physical processes which are not included in the simulations.

Within the last few years it has become possible to include a number of additional processes in such models by following, in addition to the dark matter, a dissipative gaseous component. However, even in the simplest case of a nonradiative, non–star–forming gas, the combined dark matter/gas system exhibits much more complex behaviour than a pure N–body system. In addition, such simulations are more CPU–intensive and so typically have poorer resolution than the best N–body simulations. Our current understanding of the effects of this limited resolution is still quite rudimentary. Systematic analyses of the convergence of such simulations are only just beginning (Kang et al 1994; Frenk et al, in preperation). In this paper we investigate how the finite dark matter particle mass affects the dynamics and the cooling capabilities of the gas. We show that discreteness effects give rise to a steady energy flow from the dark matter to the gas. This heating is strong enough to affect the structure of the gas within any halo made up of fewer than 1000 dark matter particles.

The outline of our paper is the following. In the next section we derive an analytic formula for the rate at which discreteness effects transfer energy from the dark matter to the gas. We compare this with the expected radiative cooling rate, we discuss how these rates scale with physical and simulation parameters, and we draw some first conclusions about how numerical simulations should be designed. In section 3 we check this analytic theory using a set of numerical simulations based on smoothed particle hydrodynamics. Simulations with and without radiative cooling are investigated separately. Section 4 discusses and summarizes our results.

2   Analytic theory

Consider a fluid element of mass m_g and density ϱ_g which is at rest. This fluid element encounters a dark matter particle of mass M_DM and relative velocity v with a closest approach distance b. In the impulse approximation (see, e.g., Binney & Tremaine 1987),

the fluid element is accelerated to velocity

$$\Delta v = \frac{2\,G\,M_{\mathrm{DM}}}{b\,v}, \tag{1}$$

or to a corresponding kinetic energy

$$\Delta E = \frac{2\,G^2\,M_{\mathrm{DM}}^2\,m_{\mathrm{g}}}{b^2\,v^2}. \tag{2}$$

This energy is dissipated to heat by shocks, by artificial viscosity, or by an adiabatic expansion of the gas to a new equilibrium state. Such encounters occur with a rate $2\pi\,v\,b\,db\,n_{\mathrm{DM}}$, so the heating rate can be written as

$$\left.\frac{dE}{dt}\right|_{\mathrm{heat}} = \int d^3v\,f(v) \int_{b_{\min}}^{b_{\max}} 2\,\pi\,db\,\frac{2\,G^2\,M_{\mathrm{DM}}\,\varrho_{\mathrm{DM}}m_{\mathrm{g}}}{b\,v}, \tag{3}$$

where $f(v)$ is the velocity distribution function for the dark matter particles. Assuming this to be Maxwellian, we obtain after the evaluation of the integrals

$$\left.\frac{dE}{dt}\right|_{\mathrm{heat}} = \sqrt{\frac{32\,\pi}{3}}\,G^2\,\ln\Lambda\,\frac{M_{\mathrm{DM}}\,m_{\mathrm{gas}}\,\varrho_{\mathrm{DM}}}{\sigma_{\mathrm{1D}}}, \tag{4}$$

σ_{1D} being the 1D velocity dispersion of the dark matter and $\ln\Lambda$ the Coulomb logarithm. For typical galaxy formation experiments $\ln\Lambda$ is in the range 3 to 7.

In an equilibrium system the internal energy of the fluid element is $E \sim 3m_{\mathrm{g}}\sigma_{\mathrm{1D}}^2/2$, so we can define a characteristic heating time by $t_h = E/(dE/dt)$, or

$$t_h = \sqrt{\frac{27}{128\,\pi}}\,\frac{\sigma_{\mathrm{1D}}^3}{G^2\,\ln\Lambda\,M_{\mathrm{DM}}\,\varrho_{\mathrm{DM}}}. \tag{5}$$

For an equilibrium dark matter dominated halo we can get a more transparent formula by comparing the heating rate near the halo half-mass radius R_h to the circular orbit period at this radius t_c. For a halo made up of N dark matter particles in total, the definitions and approximate relations, $N\,M_{\mathrm{DM}}/2 \approx 2R_h\,\sigma_{\mathrm{1D}}^2/G$, $\varrho_{\mathrm{DM}} \approx N\,M_{\mathrm{DM}}/8\,\pi\,R_h^3$, and $t_c = 2\,\pi\,R_h/\sqrt{2}\sigma_{\mathrm{1D}}$, allow us to cast equation (5) in the form

$$\frac{t_h}{t_c} = \sqrt{\frac{3}{\pi}}\,\frac{3\,N}{32\,\ln\Lambda}. \tag{6}$$

Thus for halos with around 50 dark matter particles the heating time for gas at the half-mass radius is comparable to the orbital period at that radius, and so to the halo formation time. The gas distribution within such halos will clearly never be free from substantial two-body heating effects. In a cosmological simulation, even a halo of 10^3 dark matter particles will typically have been around for several nominal formation times, and so will suffer 10 to 20% effects near its half-mass radius. Because of the strong ϱ_{DM} dependence of

equation (5), effects in the inner regions will be substantially stronger. A worrying aspect of these results is that in hierarchical clustering all massive objects build up through the aggregation of smaller collapsed systems; two-body heating must be important in the first generations of halos which form in any simulation, and it is unclear how well such early artifacts will be eliminated by later evolution.

Let us now compare the two-body heating rate with the radiative cooling rates expected for the gas in a realistic simulation:

$$\left. \frac{dE}{dt} \right|_{\text{cool}} = \varrho_{\text{g}}\, m_{\text{g}} (N_{\text{A}}\, X_{\text{H}})^2 \Lambda(T) \tag{7}$$

N_{A}, X_{H}, and $\Lambda(T)$ being Avogadro's constant, the total mass fraction of hydrogen and the cooling function, respectively. Comparing equations (4) and (7), two-body heating will dominate over radiative cooling, if

$$\sqrt{\frac{32\,\pi}{3}}\, \frac{G^2\, \ln\Lambda\, M_{\text{DM}}\, \varrho_{\text{DM}}}{\varrho_{\text{g}}(N_{\text{A}}\, X_{\text{H}})^2 \Lambda(T) \sigma_{1D}} > 1\,. \tag{8}$$

Since heating and cooling are two–body processes they both scale as ϱ^2. If we define $f \equiv \varrho_{\text{g}}/\varrho_{\text{DM}}$ and use convenient units for other quantities, we find that this inequality is equivalent to

$$M_{\text{DM}} < M_{\text{crit}} \equiv 4\ 10^9\, \sigma_{100}\, (\ln\Lambda)_5\, f_{0.05}^{-1}\, \Lambda_{-23}, \tag{9}$$

where σ_{100} is the 1D velocity dispersion in units of $100\,\text{km s}^{-1}$, $f_{0.05}$ the local baryon fraction divided by 0.05, $(\ln\Lambda)_5$ the Coulomb logarithm divided by 5, and Λ_{-23} the cooling function in units of $10^{-23}\,\text{erg cm}^{-3}$ per $(\text{H atom cm}^{-3})^2$, respectively; here we have assumed $X_{\text{H}} = 0.76$. Identifying σ_{1D} with the corresponding virial temperature, i.e., $\sigma_{100} = 1.2\sqrt{T_6}$, where T_6 is temperature in units of $10^6\,\text{K}$, we can write this critical mass in the alternative form

$$M_{\text{crit}} = 5\ 10^9\, \text{M}_\odot\, \sqrt{T_6}\, (\ln\Lambda)_5\, f_{0.05}^{-1}\, \Lambda_{-23}, \tag{10}$$

At first sight it is surprising that our critical mass turns out to be of galactic scale; only atomic and gravitational constants contribute to the right-hand-side of the inequality in equation (8), and we will see that the temperature dependence of equation (10) is quite weak over the range of interest. This "coincidence" reflects the well-known fact that the characteristic masses of galaxies appear to be determined by the condition that the cooling time for gas in a protogalactic dark halo should be comparable to the halo formation time (e.g., Rees & Ostriker 1977; White & Rees 1978). It is important to note that equation (9) is purely local and makes no specific assumptions about hydrostatic equilibrium or about the relative distributions of gas and dark matter. Only in equation (10) do we implicitly adopt such assumptions when we identify the gas temperature with the dark matter velocity dispersion. In practice, this is a weak assumption which is approximately correct in most situations of interest. We also note that our derivation is not specific to any particular numerical treatment of hydrodynamics; it depends only on the assumption that the dark matter is represented by particles of mass M_{DM}. Our critical mass should be

relevant for almost all the numerical methods currently in use to carry out cosmological hydrodynamics simulations.

The arguments given above apply only if the local cooling time is comparable to or longer than the local dynamical time. If cooling can occur on a much shorter timescale, the gas will lose its internal energy faster than the typical encounter time and two-body effects will be unable to reheat it. Such "catastrophic" cooling is unaffected by the process we are discussing. Another complication, which we will not discuss further, is that the energy deposited by an encounter may not produce local heating, but may be transported by sound waves to other regions of the system before it is dissipated.

On the basis of this analysis, we can make the following predictions for galaxy formation experiments:

- In simulations where radiative cooling is not included, energy will be steadily transferred from the dark matter to the gas. This will lead to a gradual expansion of the gas component in supposedly equilibrium systems.

- In simulations which include radiative processes but where the mass of a dark matter particle exceeds the critical value of equations (9) and (10), cooling will be suppressed wherever the cooling time is comparable to or longer than the local dynamical time (i.e., in the cooling flow regime).

Let us identify T with the virial temperature of a dark matter halo and assume gas and dark matter to be distributed similarly. For a given cooling function, we can then use equation (10) to calculate the critical mass of dark matter particles. Figure 1 shows the result as a function of T. These calculations assume a baryon fraction of 5% but are easily scaled to other values. For a cooling function appropriate to solar metallicity gas, the critical dark–matter particle mass is $\sim 10^{11}\,\mathrm{M_\odot}$ for all temperatures between 10^5 and $10^8\,\mathrm{K}$, hence for objects ranging from dwarf galaxy halos to rich galaxy clusters. Similarly, for a metallicity of $0.1\,Z_\odot$, the mass critical mass is $\sim 10^{10}\,\mathrm{M_\odot}$ for T between 2×10^4 to $5 \times 10^6\,\mathrm{K}$, the whole range relevant to galaxy halos. We therefore come to the surprising conclusion that one should use the same dark matter particle mass when simulating small galaxies as when simulating galaxy clusters. For gas of primordial composition, a realistic galaxy/cluster formation simulation requires two–body heating to be unimportant for any object with a virial temperature in the range 10^5 to $10^8\,\mathrm{K}$, implying that the dark matter particle mass should not exceed about $2\,10^9\,\mathrm{M_\odot}$. A simulation of a rich cluster would then need about half a million particles within the virial radius, a criterion which is failed by all simulations published so far. Nevertheless, for cluster simulations with several thousand particles, two–body heating times are comparable to the Hubble time only in the inner regions, so it is possible that only the core structure of the gas is affected by numerical artifacts. Figure 1 also shows a cooling function due to bremsstrahlung alone. This approximates the extreme case of cooling in the presence of a strong UV background, where collisionally excited line emission can be almost completely suppressed (e.g., Efstathiou 1992). In this case, $\Lambda \propto \sqrt{T}$, and so $M_{\mathrm{crit}} \propto T$. For a dwarf galaxy ($T_{\mathrm{vir}} = 10^5\,\mathrm{K}$), dark
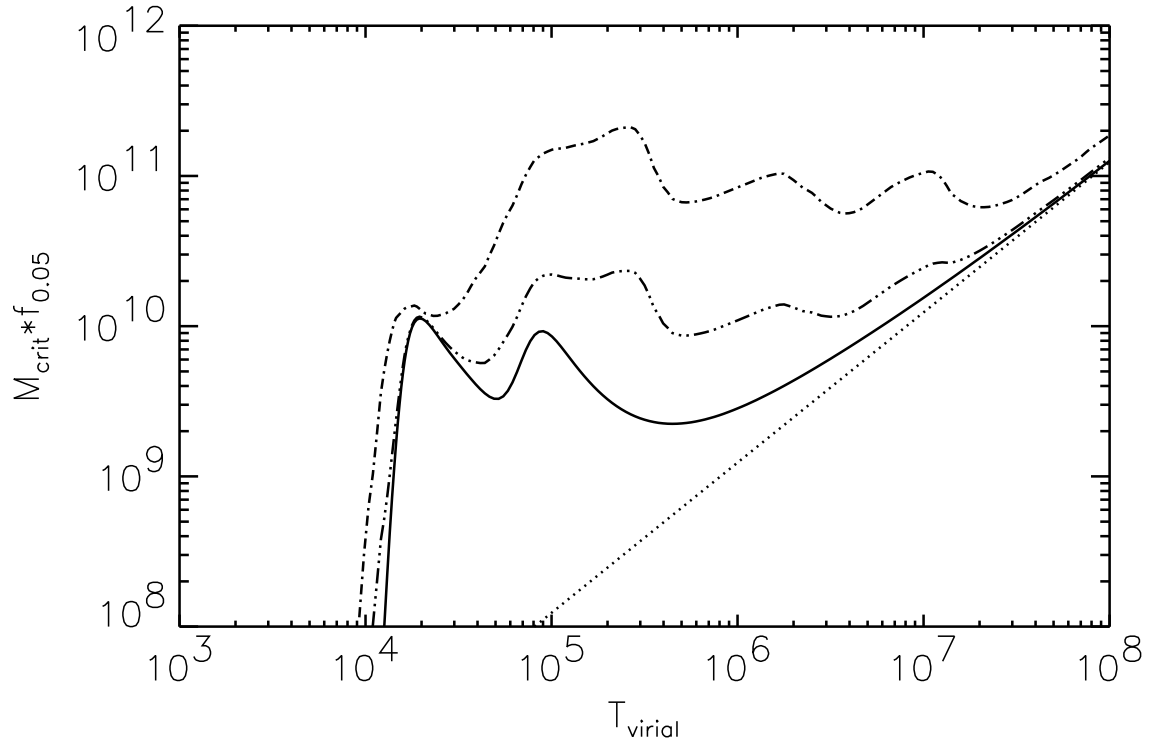
Figure 1: Critical mass for dark matter particles (according to equation (10)) as a function of the virial temperature of the simulated system. The different curves correspond to different cooling functions: primordial composition (solid line), solar metallicity (dashed–dotted), $\frac{1}{10}$ of solar metallicity (dashed–triple dotted), and pure bremsstrahlung (dotted).

matter particle masses are required to be below $10^8 \, \mathrm{M}_\odot$, i.e., the galaxy halo should be represented by several hundred particles.

Finally we note that M_{crit} is the value of the dark matter particle mass for which radiative cooling and artificial two–body heating are equal. To get realistic results any numerical simulation should use particle masses which are at least a factor of two or three smaller than M_{crit}.

3   Numerical verification

In the previous section we concluded that for parameters typical of current galaxy formation experiments, two–body heating can substantially affect the properties of the gas. We predict that in simulations without cooling the gas in equilibrium systems will slowly expand, while in simulations that include radiative losses the gas may still be prevented from cooling where it should. In this section we will test these predictions by means of some numerical experiments. These were performed using the smoothed particle hydrodynamics code GRAPESPH (Steinmetz 1996). We choose initial conditions which are relevant for galaxy formation simulations but which also allow easy control over experimental parameters. In particular, we choose the initial conditions proposed by Katz (1991): a homogeneous, overdense, and rigidly rotating sphere of total mass $8.1 \times 10^{11} \, \mathrm{M}_\odot$ with superposed small-scale density fluctuations drawn from a CDM power spectrum. The evolution was simulated with different particle numbers, $N = 250, 500, 1000, 4000$ and 17000. The initial conditions for the lower resolution simulations were obtained by random sampling those of the model with 17000 particles. This object collapses at $z \sim 2$ but the simulations were followed over a Hubble time and the structure was analysed only after $z = 1$ when gas and dark matter have relaxed and are approximately in equilibrium. For simulations including cooling, the cooling was switched on only after $z = 1$. (Throughout we assume $\Omega = 1$ and $H_0 = 50 \ \mathrm{km \ s^{-1} \, Mpc^{-1}}$.) The density profiles of the relaxed system have $\varrho \propto r^{-2}$ between 20 and 90 kpc; the profile is steeper at larger and shallower at smaller radii, resembling the "universal" halo structure proposed by Navarro, Frenk & White (1996). The gas temperature is almost uniform within 50 kpc, but drops at larger radii.

3.1   Simulations without cooling

In Figure 2 we show the cumulative mass profiles for gas and dark matter in simulations with differing resolution. The dark matter profiles show no significant evolution in any of these models. (The fluctuations at small radii for $N = 250$ are just statistical noise.) In contrast, the gas distribution expands substantially for $N = 250$, but only slightly for $N = 4000$. To demonstrate that this expansion reflects the mass of the dark matter particles we also show a simulation with 250 gas particles and 4000 dark matter particles, i.e., gas and dark matter particles have roughly the same mass. In this case the expansion of the gas component is again small, and with the exception of noise effects at very small radii, the gas profile is compatible with that obtained using 4000 gas particles.
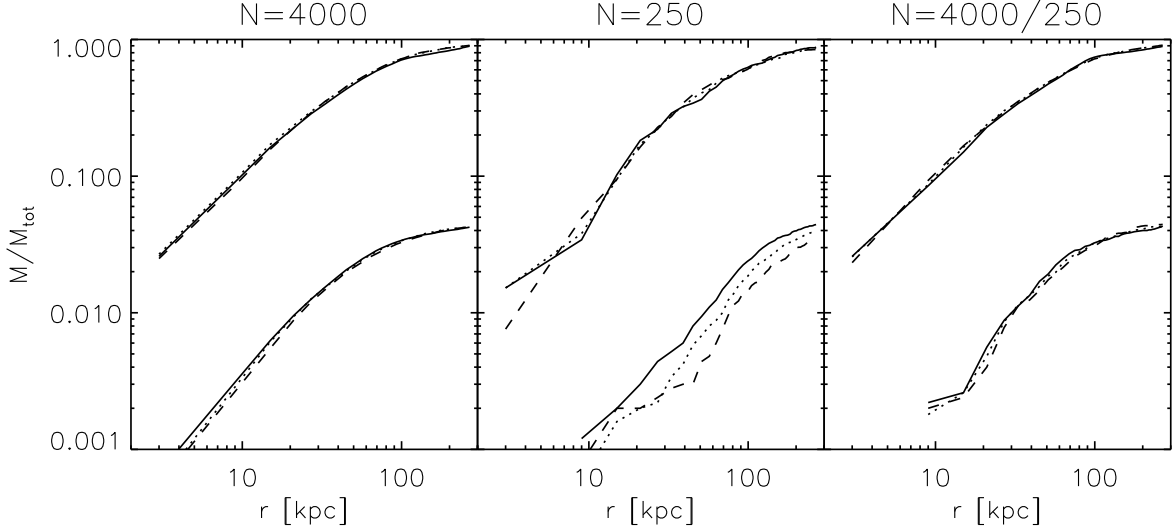
7

Figure 2: Time evolution of the cumulative mass profiles for dark matter (upper curves) and gas (lower curves) for three different resolutions: 4000 particles in each component (left), 250 particles in each component (middle), and 250 gas particles but 4000 dark matter particles (right). The curves represent epochs 0 Gyr (solid), 4 Gyr (dotted) and 8 Gyr (dashed) after hydrostatic equilibrium has been established.

It is also instructive to look at the heating of the gas in terms of its entropy evolution. After hydrostatic equilibrium is established, the specific entropy $s = \ln(T^{1.5}/\varrho)$ of a gas particle should be constant $\frac{d}{dt}s = 0$. As shown in Figure 3, this is indeed the case for the $N = 17000$ run. There is an almost perfect linear relation between initial and final entropy. This also demonstrates that for high particle numbers the amount of spuriously generated entropy due to the artificial viscosity is negligible. Only at very large radii a slight scatter can be seen, which can be explained by some dynamical evolution close to the virial radius. For smaller particle numbers, an evolution in s becomes visible: when $N = 1000$ only particles with the lowest entropies are affected, while for $N < 500$ the whole system is affected. The low entropy gas exhibits the strongest evolution because it lies near the center of the halo and so has the shortest heating time. Comparison with the 250/4000 and 1000/17000 models shows that entropy generation is not significantly affected by numerical resolution in the gas component, but is determined primarily by the mass resolution of the dark matter component: lowering the mass of the dark matter particles at constant gas resolution suppresses the artificial heating. Note that two–body heating also occurs when dark matter particle masses are smaller than those of fluid elements since, unlike the standard stellar dynamical case, the fluid elements are at rest when the system is in equilibrium.
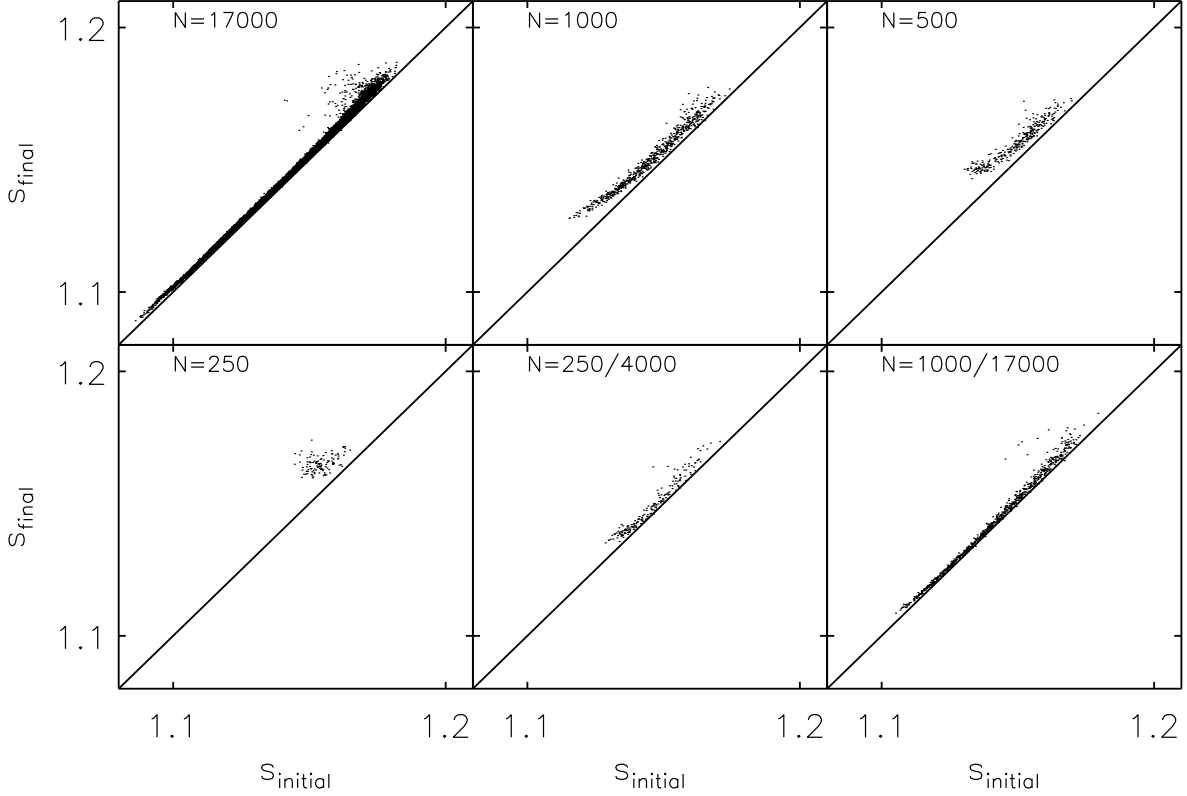
Figure 3: Initial versus final specific entropy (in units of $(N_A\,k_b)$) of gas particles for simulations with (from top left to bottom right) 17000, 1000, 500, 250 particles in each of the two components, and with 250/4000 and 1000/17000 gas/dark matter particles.

3.2 Simulations with cooling

We now consider simulations which include radiative cooling. To simplify comparison of our simulations with the predictions of our analytic model, we use a schematic cooling function for which $\Lambda = $ const above a lower cutoff of 10^4 K. As mentioned above, we switch cooling on only after the initial relaxation phase. Thus the phase we analyse begins with a relaxed halo, in which the gas has the virial temperature and is in hydrostatic equilibrium within the dark matter potential well. We choose Λ to be relatively small so that we can demonstrate two–body heating effects clearly using about 1000 particles. Statistical noise then has little effect on our conclusions. These physical conditions are similar to a cooling flow. We took the mass of a dark matter particle to be $7.7\ 10^8\,M_\odot$, assumed a gas fraction of 5%, and performed two simulations, one with $\Lambda_{-23} = 0.4$, the other with $\Lambda_{-23} = 0.1$. The half-mass radius of the collapsed system is then 60 kpc, while the gravitational softening is 5 kpc giving a Coulomb logarithm of about 2.5. According to equation 10, for the appropriate virial temperature, $T_6 = 1.5$, our chosen particle mass corresponds to the critical value for a cooling coefficient of $\Lambda_{-23} = 0.25$, midway between those of our two simulations. We expect, therefore, that in one of these two models the gas
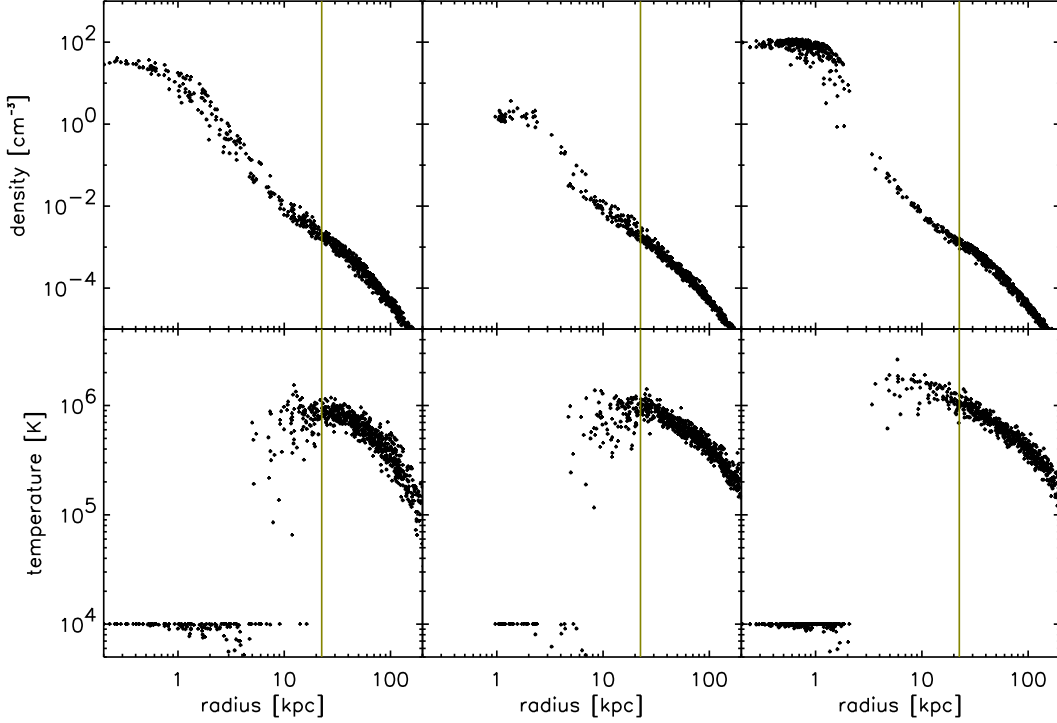
9

Figure 4: Density (top) and temperature (bottom) as a function of radius for two simulations starting from identical initial conditions but with $\Lambda_{-23} = 0.4$ (left) and $\Lambda_{-23} = 0.1$ (middle). These simulations have evolved for the same number of cooling times since virialisation. The simulation on the right has the same number of gas particles but 17 times more dark matter particles. Its evolution time and Λ_{-23} value are identical to those of the model in the middle column. The vertical dotted line corresponds to the radius where the cooling time of the initial model equals the time for which cooling was allowed.

will be able to cool while in the other it will not. The two simulations were run for the same number of nominal cooling time scales, i.e., the model with the lower cooling coefficient was run for a correspondingly longer time. In both cases the final cooling radius should be about 23 kpc implying that about 16 per cent of the gas should be able to cool. For an additional comparison we also consider a second model with $\Lambda_{-23} = 0.1$ which differs from the first only in that the dark matter is represented by 17000 particles. Thus two–body heating effects are suppressed by a factor of 17.

In Figure 4 we show density and temperature profiles for the final states of the three simulations. In the model with $\Lambda_{-23} = 0.4$ almost all the gas within the cooling radius has started to cool, and a large fraction has already settled at 10^4 K, the cutoff of the assumed cooling function. The gas distribution responds dynamically to this cooling. The density near the center has already increased by three orders of magnitude. The situation is different when $\Lambda_{-23} = 0.1$. Although the simulation has evolved for the same number of cooling times, only those particles which where dense enough to cool catastrophically

10

($t_{\rm cool} \lesssim t_{\rm dyn}$) have cooled and the density has only increased by an order of magnitude. Almost no gas in the cooling-flow regime ($t_{\rm dyn} < t_{\rm cool} < t_{\rm Hubble}$) has cooled down and the total fraction of cooled gas is reduced by a factor of 2. Increasing the number of dark matter particles without altering the cooling eliminates this difference (Fig. 4, right). Again all gas within the cooling radius can cool and and settles to a distribution similar to the $\Lambda_{-23} = 0.4$ run. Since more dynamical times are now available to react to the loss of pressure support, and since the central potential cusp of the dark halo is now better defined, the central gas density increases even more dramatically in this case. These experiments show impressively how two–body heating can alter the dynamics and thermodynamics of the gas, especially in a cooling flow situation.

4   Summary and Discussion

We have analyzed how two–body encounters between fluid elements and dark matter particles can lead to spurious heating of the gas component in galaxy formation experiments. We have shown both analytically and numerically that this process can affect not only the thermodynamic state, but also the dynamics of the gas. Our analytic work establishes an upper bound to the mass of a dark matter particle for two–body heating to be subdominant when simulating any given physical situation. Our numerical simulations show that the predicted effect is indeed present, and that the critical mass of equation (10) provides a reliable guide for designing numerical experiments so that two–body heating does not cause a qualitative change in their outcome. Simulations of cooling flows and of galaxies forming in the presence of a strong UV background are particularly susceptible to two-body heating, and must therefore be designed with particular care.

Although the effect we have discussed is not important in the catastrophic cooling regime, numerical simulations have shown that when cooling occurs only in this regime, and no additional physics is included, it is not possible to make galaxy disks as large as those observed. Disk-like objects do form but have too little angular momentum and so are too concentrated (Navarro & Benz 1991, Navarro & White 1994, Navarro & Steinmetz 1996). Furthermore, the observed specific angular momenta of giant spiral disks are so large that they must have formed late and so most plausibly in the cooling flow regime (e.g., White 1991). The solution to this problem may be, as is usually claimed, that feedback from stellar evolution is an indispensable ingredient of galaxy formation; such feedback could delay the condensation of gas so that most of it cools late, and with relatively little loss of angular momentum to the dark matter. Current semi-analytic models include a treatment of such feedback processes and suggest that a substantial fraction of the matter in the present galaxy population may have condensed in the quasi-cooling-flow regime (White & Frenk 1991, Kauffmann, Guiderdoni & White 1993; Fabian & Nulsen 1994). Thus, those numerical simulations which, as a result of poor resolution, avoided excessive catastrophic cooling at early times, may nevertheless have missed an important ingredient of galaxy formation because of of two-body heating, in particular, the physics most relevant to the formation of spiral disks.

Our findings lead us to conclude that the common practice of using the same number of dark matter and gas particles in cosmological and galaxy formation simulations may be unwise. The computing time spent per gas particle is usually much higher than for a dark matter particle, especially if a multiple time-step scheme is used. It may, therefore, be advantageous to use several times more dark matter particles than gas particles. The total CPU time will be only moderately increased while two-body heating can be suppressed by a substantial factor.

Many simulations of individual galaxies and clusters apply a multi-mass technique (Porter 1985; Katz & White 1993; Navarro & White 1994) in which the tidal field due to surrounding matter is represented by a relatively small number of massive particles. These massive particles are supposed to stay outside the high resolution region of interest. If, however, some of them accidently pass through a forming galaxy, our experiments demonstrate that they may prevent cooling of low density gas. It is, therefore, important that simulations which use such techniques should be checked to ensure that contamination by massive particles is kept to an acceptably low level.

Although our numerical experiments have used smoothed particle hydrodynamics, our analytic theory makes no assumption about the underlying numerical technique other than that the dark matter is represented by discrete particles, and that sound waves and shocks generated in the gas component will be dissipated as heat. As a result, the considerations of this paper should apply to all the techniques currently used to simulate cosmological hydrodynamics and galaxy formation.

References

Binney J, Tremaine S, 1987, *Galactic Dynamics* Princeton University Press

Efstathiou G, 1992, MNRAS, 256, 43p

Efstathiou G, Davis M, Frenk C S, White S D M, 1995, ApJS, 57, 241

Efstathiou G, Davis M, Frenk C S, White S D M, 1988, MNRAS, 235, 715.

Fabian A C, Nulsen P E J, 1994, MNRAS, 269, p33

Kang H, et al., 1994, ApJ, 430, 83

Katz N, 1991, ApJ, 368, 325

Katz N, White S D M, 1993, ApJ, 412, 455

Kauffmann G, Guiderdoni B, White S D M, 1993, MNRAS, 264, 201

Navarro J F, Benz, 1991, ApJ, 380, 320

Navarro J F, Steinmetz M, 1996, ApJ, submitted

Navarro J F, White S D M, 1994, MNRAS, 267, 401

Navarro J F, Frenk C S, White, S D M, 1996, ApJ, 462, 563.

Porter D, 1985, PhD thesis UC Berkeley

Rees M J, Ostriker J P, 1977, MNRAS, 179, 541

Steinmetz M, 1996, MNRAS, 278, 1005

White S D M, 1991, in The Dynamics of Galaxies and their Molecular Cloud Distributions, Combes F, Casoli F eds, Reidel, p383.

White S D M, Frenk C S, 1991, ApJ, 379, 52

White S D M, Rees M J, 1978, MNRAS, 183, 341